

Simulating quantum circuits using efficient tensor network contraction algorithms with subexponential upper bound

Thorsten B. Wahl¹ and Sergii Strelchuk¹

¹*Department of Applied Mathematics and Theoretical Physics,
University of Cambridge, Wilberforce Road, CB3 0WA, United Kingdom.*

(Dated: August 3, 2022)

We derive a rigorous upper bound on the classical computation time of finite-ranged tensor network contractions in $d \geq 2$ dimensions. By means of the Sphere Separator Theorem, we are able to take advantage of the structure of quantum circuits to speed up contractions to show that quantum circuits of single-qubit and finite-ranged two-qubit gates can be classically simulated in subexponential time in the number of gates. In many practically relevant cases this beats standard simulation schemes. Moreover, our algorithm leads to speedups of several orders of magnitude over naive contraction schemes for two-dimensional quantum circuits on as little as an 8×8 lattice. We obtain similarly efficient contraction schemes for Google’s Sycamore-type quantum circuits, instantaneous quantum polynomial-time circuits and non-homogeneous (2+1)-dimensional random quantum circuits.

I. INTRODUCTION

Tensor network methods are a single most impactful toolkit responsible for some of the most dramatic improvements in a large number of areas of physics and computer science. They revolutionized our understanding of condensed matter physics [1, 2], lattice field theories [3–7], quantum information and computing [8–15], and machine learning [16], achieving results which are far out of reach for analytical methods. Recently, Google exhibited a quantum computational device capable of reaching quantum advantage – by presenting a highly unstructured computational task which would reportedly take an exceptionally long time on a classical computer to solve [17]. In the absence of a formal proof of hardness, this challenge spurred a number of exciting developments on the classical algorithms side with the aim to find an efficient solution by classical means [18–20]. Tensor network contraction methods coupled with ingenious empirical contraction strategies exhibited their immense power reducing the classical computational time to mere hours and even minutes [21–23].

The quest for an efficient solution using tensor networks allows one to develop new contraction techniques and intuition about the problem instance. Alas, the resulting simulation algorithm does not typically allow us to solve generic problems in this class efficiently: a slightly tweaked computational task – whilst still being easy for a quantum computer – can invalidate the speedup obtained by classical simulation algorithms in this case. This presents one of the major problems when applying tensor network methods: the lack of analytical guarantees for contraction that work well for a range of problems in the class. Efficient empirical approaches that work well for a particular problem instance may comprehensively fail, forcing one to start the search for an efficient simulation method from a clean slate by a costly path of trial and error.

Clearly, little can be done analytically when the under-

lying problem is unstructured, i.e. the quantum circuit is made up of uniformly random gates acting on a random subset of qubits. However, as noted in Ref. [24], this model is not representative of practical quantum computational processes – quantum algorithms expressed in the circuit model yield circuits which are far from uniformly random. Considering circuit topology and the ‘macroscopic’ structure (or layout) of quantum circuits can provide us with valuable extra information which may subsequently be used to derive efficient quantum simulation algorithms. We develop a method which allows us to take advantage of the circuit structure and thus for the first time yields tensor network contraction algorithms with nontrivial theoretical runtime guarantees. This method is based on the idea contained in a rich class of so-called separator theorems [25, 26]. In their simplest form, they represent isoperimetric inequalities for planar graphs. Such (planar) separator theorems state that any planar graph can be split into smaller subgraphs by removing a fraction of its vertices. More precisely, removing $O(\sqrt{n})$ vertices from a graph with n vertices partitions it into disjoint subgraphs each of which has at most $2n/3$ vertices. The Planar Separator Theorem [25] (for $d = 2$) has found uses in classical complexity theory – counting satisfiability problems ($\#SAT$) problems and $\#Cubic\text{-Vertex-Cover}$, where it was decisively better than the state-of-the-art solvers [27] and Boolean symmetric functions [19], and has been mentioned in the context of quantum circuits [28]. We apply the ideas outlined in separator theorems to derive analytical upper bounds on the classical simulation times of quantum circuits taking into account the explicit layout of each of the quantum circuits. Recently, the authors of Ref. [29] argued that (assuming the Strong Exponential Time Hypothesis) strongly simulating certain $poly(n)$ depth quantum circuits on n qubits requires an $2^{n-o(n)}$ time using tensor network methods. Our work rigorously demonstrates how one can derive a constructive tensor-contraction method with subexponential upper bounds on its runtime if we take advantage of extra information

about the structure of the circuit.

This article is structured as follows: In Section II we give a very brief introduction to the types of tensor network contractions that appear in the range of practical applications, emphasizing their ‘metadata’ which will be incorporated in the algorithm. Thereafter, we recall the Sphere Separator Theorem [26] and use it to prove a rigorous upper bound on the classical contraction time of $d \geq 2$ -dimensional tensor networks. In Section III we demonstrate the power of this result (alongside the discussion of a class of Planar Separator Theorems [25]) for quantum circuit simulations, obtaining analytical guarantees on their classical simulation times. We also review an algorithm [26] that can be used to efficiently determine the contraction order underlying the Sphere Separator Theorem in Section IV. Finally, in Section V we consider several examples, for which we numerically demonstrate the advantage provided by our analytical guarantees over naive contraction schemes for sufficiently large systems that arise in practical applications, highlighting the powerful technique based on the Sphere Separator Algorithm, which leads to tremendous speedups for modest system sizes. We conclude the article in Section VI, where we discuss broader implications of our theoretical results as well as hint towards further possible improvements when combined with the established heuristic contraction schemes.

II. TENSOR NETWORK CONTRACTIONS

We now provide a short overview of the conventional graphical representation of tensor networks and propose an alternative one, useful for our purposes. Based on the latter, we then employ the Sphere Separator Theorem to prove an upper bound on the classical contraction time of arbitrary tensor networks in $d \geq 2$ dimensions to a scalar, which allows us to calculate the relevant expectation values.

In applications of tensor networks, their graphical short-hand notation has become indispensable. Conventionally, a rank- m tensor is represented by a box or a sphere (or, as in our work, by a dot) with m emanating lines. Each line corresponds to one tensor index and a line connecting two tensors to a contraction (i.e., a summation) of the corresponding index, see Fig. 1a,b.

We consider the contraction of a d -dimensional tensor network ($d \geq 2$) of n tensors to a scalar. Below, we derive an upper bound on the classical computation time of the tensor network contraction with the following theorem as our main tool:

Sphere Separator Theorem (SST) [26]. *For a set of n spheres in d dimensions such that each point is contained in at most k spheres the following holds: There exists a sphere S such that removing the set $\Gamma_O(S)$ of spheres which S intersects with gives rise to two mutually*

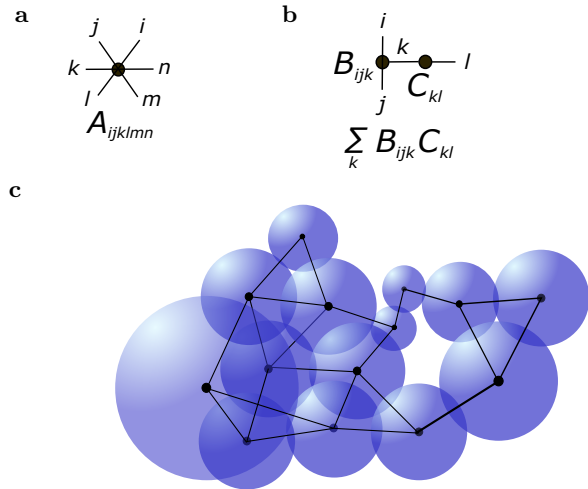


FIG. 1. a: Conventional graphical representation of a tensor as a dot with emanating lines, each corresponding to one tensor index. b: The lines connecting two tensors correspond to contracted indices. c: The conventional graphical representation is replaced by a new one, where each tensor is endowed with a sphere, and only intersecting spheres *can* correspond to tensors with one contracted index. In the shown example, up to $k = 3$ spheres overlap at any point.

non-intersecting sets of spheres $\Gamma_E(S)$ and $\Gamma_I(S)$ with

$$|\Gamma_O(S)| \leq c_d k^{1/d} n^{1-1/d}, \quad (1)$$

$$|\Gamma_E(S)|, |\Gamma_I(S)| \leq \frac{d+1}{d+2} n. \quad (2)$$

The coefficients are $c_1 = 1$, $c_2 = 2$, $c_3 < 2.135$, $c_4 < 2.280$, $c_5 < 2.421$, and in general $c_d < \sqrt{2d/\pi} [1 + \mathcal{O}(1/\log(d))]$ for $d > 1$ [30].

We make use of SST to derive a new bound on the contraction complexity of a tensor network which takes into account the information about its connectivity:

Theorem 1. *We consider the full contraction of a d -dimensional tensor network ($d \geq 2$) of n tensors of at most M entries each. We assume in a graphical representation of the tensors as spheres of radii such that only if two tensors correspond to intersecting spheres they can have one contracted index, the maximum number k of spheres overlapping in any point is n -independent (finite-ranged tensor network). Then, for sufficiently large n , the classical computation time of the tensor network contraction is upper bounded by $2^{-d} \left(\frac{n}{c_d^k}\right)^{\lceil \log_2 \left(\frac{d+2}{d+1}\right) \rceil - 1} M^{a_d k^{1/d} n^{1-1/d}}$, where $a_d = c_d / \left[2 - 2 \left(\frac{d+1}{d+2}\right)^{1-1/d}\right]$.*

The conversion of the conventional graphical representation of tensor networks to the one above in terms of spheres is illustrated in Fig. 1c.

Proof: We use the SST to split the tensor network into two disconnected tensor networks of at most $n(d+1)/(d+$

2) tensors each [corresponding to $\Gamma_{E,I}(S)$] and the tensors sitting at the interface $\Gamma_O(S)$. These are then included into those two tensor networks such as to minimize the overall dimension of the bonds between them. As a result, the bond dimension contributed by each of the tensors at the interface is at most $M^{1/2}$. We iteratively apply this procedure to the resulting two sets until all sets are of size $\mathcal{O}(n^{1/d})$ (where the upper bounds for $|\Gamma_O(S)|$ and $|\Gamma_{E,I}(S)|$ are of the same order), obtaining a separator hierarchy (i.e. a recursive decomposition into smaller chunks). Let ℓ be the level of the separator hierarchy and $T_{i_1 i_2 \dots i_\ell}^{(\ell)}$ be the corresponding tensor networks with the indices $i_j = 0, 1$ indicating the path taken through the separator hierarchy (see Fig. 2). If we assume that $T_{i_1 \dots i_\ell}^{(\ell)}$, viewed as a tensor, has $M_{i_1 \dots i_\ell}^{(\ell)}$ entries, the computational time to create $T_{i_1 \dots i_\ell}^{(\ell)}$ (in appropriate units) is

$$t(T_{i_1 \dots i_\ell}^{(\ell)}) \leq \min \left[t(T_{i_1 \dots i_{\ell-1} 0}^{(\ell+1)}) + t(T_{i_1 \dots i_{\ell-1} 1}^{(\ell+1)}) + M_{i_1 \dots i_\ell}^{(\ell+1)}, M_{i_1 \dots i_\ell}^{(\ell)} \right], \quad (3)$$

where $M_{i_1 \dots i_\ell}^{(\ell+1)}$ denotes the product of the dimensions of all of the indices of the tensors $T_{i_1 \dots i_{\ell-1} 0}^{(\ell+1)}$ and $T_{i_1 \dots i_{\ell-1} 1}^{(\ell+1)}$, counting shared indices once. By the SST, $M_{i_1 \dots i_\ell}^{(\ell+1)} \leq M^{\frac{1}{2} \sum_{j=1}^{\ell+1} c_d k^{1/d} [n(\frac{d+1}{d+2})^{j-1}]^{1-1/d}}$, as the sum in the exponent is the maximum number of constituting tensors which can sit at the combined surface of the tensor networks $T_{i_1 \dots i_{\ell-1} 0}^{(\ell+1)}$ and $T_{i_1 \dots i_{\ell-1} 1}^{(\ell+1)}$ (counting the surface separating them once), and $M^{1/2}$ is the maximum bond dimension per tensor. Repeatedly inserting Eq. (3) into itself yields the closed form

$$t(T^{(0)}) \leq \sum_{\ell=0}^{z-1} 2^\ell M^{\frac{1}{2} \sum_{j=1}^{\ell+1} c_d k^{1/d} [n(\frac{d+1}{d+2})^{j-1}]^{1-1/d}} + 2^z M^{\mathcal{O}(n^{1/d})}, \quad (4)$$

where z is the level of the separator hierarchy where generating the constituting tensor networks from scratch by brute-force contraction will be computationally cheaper [leading to the right term in Eq. (4)] than the cost given by the bound in Eq. (1). After upper bounding the sum in the exponent of Eq. (4) by an infinite, i.e., geometric, sum, we obtain

$$t(T^{(0)}) < 2^z M^{\frac{c_d k^{1/d}}{2-2(\frac{d+1}{d+2})^{1-1/d}} n^{1-1/d}} \quad (5)$$

for sufficiently large n . By the definition of z , we have $c_d k^{1/d} [n(\frac{d+1}{d+2})^z]^{1-1/d} = n(\frac{d+1}{d+2})^{z+1}$, and thus $z = \log_2(\frac{n}{c_d^d k}) / \log_2(\frac{d+2}{d+1}) - d$, giving the stated result. \square

When the underlying interaction graph is planar, a more appropriate tool is an analogue of the SST – the Planar Separator Theorem [25]:

Planar Separator Theorem (PST) [25]. *A planar graph, i.e., a two-dimensional graph of non-intersecting*

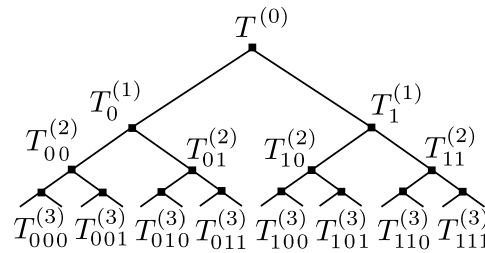


FIG. 2. Separator hierarchy: The original tensor network $T^{(0)}$ gets successively split into smaller tensor networks $T_{i_1 \dots i_\ell}^{(\ell)}$.

lines and n vertices, can be separated into two disconnected graphs of at most $2n/3$ vertices each by removing $c_{PST}\sqrt{n} + \mathcal{O}(1)$ vertices with $c_{PST} < 1.971$ [31].

However, in Refs. [19, 27] the exponent in Eq. (5) was not calculated; in particular, it was not clear if it is still of order $\mathcal{O}(\sqrt{n})$ when one takes the entire separator hierarchy into account. After evaluating the expression corresponding to Eq. (4) below, we obtain an improved upper bound of $t(T^{(0)}) < 0.25(n/c_{PST}^2)^{\lceil \log_2(3/2) \rceil - 1} M^{a_2' \sqrt{n}}$ with $a_2' = c_{PST}/(2-2\sqrt{2/3}) < a_2 = c_2/(2-2\sqrt{3/4})$ for $d = 2$.

III. CLASSICAL SIMULATION OF QUANTUM CIRCUITS

We now apply ideas of the SST and the PST to derive analytical guarantees on the classical simulation times of quantum circuits taking into account the explicit layout of each of the quantum circuits.

Consider a quantum circuit U of single-qubit and finite-ranged two-qubit gates acting on N qubits over T time steps. For simplicity, we assume that the system is initialized in the $|00 \dots 0\rangle := |\mathbf{0}\rangle$ state. We represent the expectation value c of the measurement result $P = \bigotimes_i P_i$, where P_i is a projector on qubit i , as a tensor network, $c = \langle \mathbf{0} | U^\dagger \bigotimes_i P_i U | \mathbf{0} \rangle$. Two-qubit gates correspond to rank-4 tensors and single-qubit gates to rank-2 tensors (unitary matrices). The latter as well as the P_i can be absorbed into the former, such that only the two-qubit gates affect the scaling of computational complexity:

Theorem 2. *The classical simulation time of a $(d+1)$ -dimensional quantum circuit with $d \geq 2$ of single- and two-qubit gates of maximum range l and N qubits of minimal distance r apart scales at most as*

$$\left[\sum_{i=1}^N f(\mathbf{x}_i) \right]^{\lceil \log_2(\frac{d+2}{d+1}) \rceil - 1} 2^{8a_d(1+l/r)F^{1/d}} \left[\sum_{i=1}^N f(\mathbf{x}_i) \right]^{1-1/d},$$

where $f(\mathbf{x}_i)$ is the number of two-qubit gates acting on the qubit i at position $\mathbf{x}_i \in \mathbb{R}^d$ and $F = \max_i f(\mathbf{x}_i)$. For $d = 2$ and nearest neighbor two-qubit gates ($l = r$), a tighter bound scales as

$$\left[\sum_{i=1}^N f(\mathbf{x}_i) \right]^{\lceil \log_2(3/2) \rceil - 1} 2^{4a_2' \sqrt{\sum_{i=1}^N f(\mathbf{x}_i)} [2+f(\mathbf{x}_i)]/2}.$$

Proof: We first split the two-qubit gates using a singular value decomposition into a contraction of two rank-3

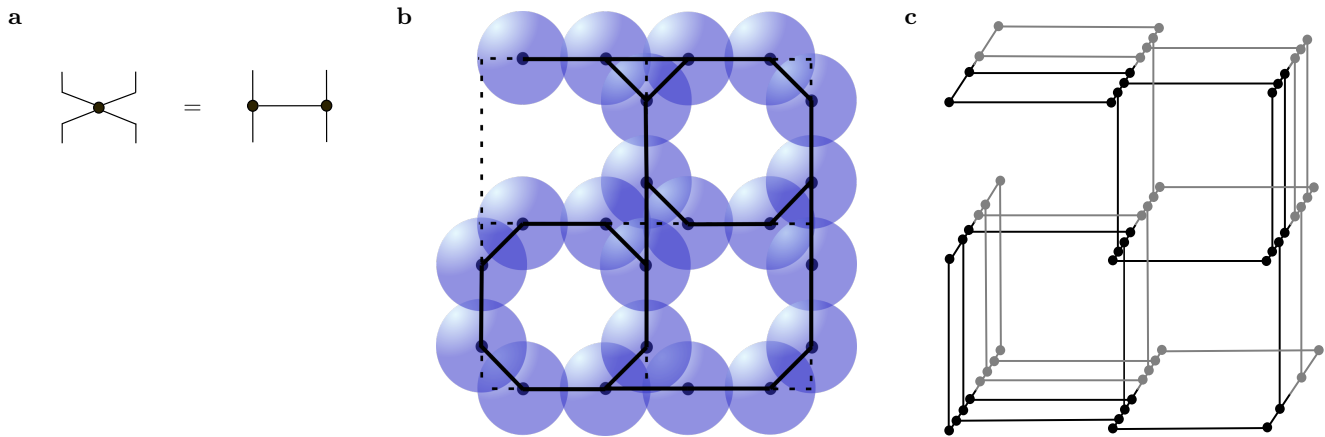


FIG. 3. a: Singular value decomposition of the tensor corresponding to a two-qubit gate into two rank-3 tensors (represented as dots), where the diagonal matrix containing the singular values has been absorbed into one of the rank-3 tensors. The connecting line has dimension 4, while all other lines represent dimension 2 indices. b: Collapse of the $(d + 1)$ -dimensional tensor network corresponding to a quantum circuit onto d -dimensional space. In the Figure, $d = 2$, and the qubits are arranged on a 3×3 square lattice (dashed lines) with nearest-neighbor gates. The tensor network contraction is graphically represented both in the conventional way by lines connecting vertices and in the way introduced in this work in terms of spheres surrounding tensors. Note that the collapse of the time dimension causes tensors (and spheres) to lie on top of each other. c: Collapse of the $(d + 1)$ -dimensional tensor network onto d -dimensional space with the time direction corresponding to slightly offset tensors for clarity, shown in the conventional graphical representation. Tensors coming from the (adjoint) unitary $U^{(\dagger)}$ are drawn in black (gray). In order to convert this graphical representation to a planar graph, vertices have to be placed at the intersection points.

tensors, see Fig. 3a. We collapse the time axis to length zero, such that the positions of all tensors are given by spatial coordinates only. Each gate acting on qubits i and j gives rise to two tensors, which we place at positions $\mathbf{x}_i + (\mathbf{x}_j - \mathbf{x}_i)/4$ and $\mathbf{x}_j + (\mathbf{x}_i - \mathbf{x}_j)/4$, respectively. We choose the surrounding spheres to have radius $l/4 + \epsilon$ ($\epsilon > 0$), such that all connected tensors correspond to intersecting spheres, see Fig. 3b. In Theorem 1, we have $n = 2 \sum_{i=1}^N f(\mathbf{x}_i)$ tensors (coming from U and U^\dagger). Each point in space is only covered by spheres whose origins are at a distance $\leq l/4 + \epsilon$. As $r/2$ is the minimal distance between the centers of the spheres of different qubits, we therefore have $k \leq 2F \left(\frac{l/4 + r/4}{r/4} \right)^d$. With Theorem 1 and since the number of entries of each tensor is $M = 16$, we obtain the stated scaling. For $d = 2$ and nearest-neighbor two-qubit gates, we can use the PST after transforming our graph to one whose vertices are connected by non-intersecting lines: Going back to the conventional graphical representation, we displace the tensors corresponding to the same qubit but to different times by $\epsilon' > 0$ with respect to each other, see Fig. 3c. In the limit $\epsilon' \rightarrow 0$ there can be up to $[f(\mathbf{x}_i)]^2/2$ intersections between the lines connecting the tensors around the qubit at \mathbf{x}_i to tensors around neighboring qubits (the lines of $f(\mathbf{x}_i)/2$ gates applied at an earlier time intersecting with $f(\mathbf{x}_i)$ lines of gates from a later time and the corresponding adjoint operation). We can transform this graph to a planar graph by placing vertices (identity tensors) at the corresponding intersection points, resulting in $n \leq \sum_{i=1}^N (2f(\mathbf{x}_i) + [f(\mathbf{x}_i)]^2/2)$ vertices overall. The

identity tensors placed at the intersection points have $M = 4^4$ entries, and we thus obtain the stated tighter bound. \square

As $\sum_{i=1}^N f(\mathbf{x}_i) \leq NF$, the above bounds generally beat left-to-right contraction: for example, for a hypercubic L^d lattice with nearest neighbor two-qubit gates, left-to-right contraction yields a bound $t_{\text{side}} \leq 2^{4FL^{d-1}} L = 2^{4FN^{1-1/d}} N^{1/d}$. This is larger than the bounds of Theorem 2 for a very inhomogeneous $f(\mathbf{x})$, which, for instance, is commonly the case in quantum error correction. Similarly, those bounds improve over the classical simulation time of explicit time evolution $t_{\text{expl}} \leq T2^N$ if $F < N^{1/d}/[8a_d(1 + l/r)]$.

IV. NUMERICAL IMPLEMENTATION

The proof of the SST is constructive [26], and there also exists an algorithm to efficiently calculate the corresponding sphere separator. Here we show how this algorithm can be used to compute a separator hierarchy satisfying the bounds of Theorems 1 and 2. We will see in Section V that the separator hierarchies obtained in practice correspond to much lower classical runtimes.

The algorithm to calculate the sphere separators of Theorem 1 and 2 is a probabilistic approach and was first presented in Ref. [26]. In our case, Algorithm 1 (summarized below) has to be applied $\mathcal{O}(n)$ times. $|\Gamma_{\mathcal{O}}(S)|$ allows us to provide an upper bound on the classical simulation time of the specific quantum circuit Algorithm 1

Algorithm 1: Sphere Separator
Algorithm [26]

Input: Positions $\mathcal{P} = \{\mathbf{p}_1, \mathbf{p}_2, \dots, \mathbf{p}_s\} \in \mathbb{R}^d$ of centers of spheres, representing s tensors, and the corresponding radii $\mathcal{R} = \{r_1, r_2, \dots, r_s\}$.

- 1: Compute $\Pi(\mathcal{P}) = \{\Pi(\mathbf{p}_1), \Pi(\mathbf{p}_2), \dots, \Pi(\mathbf{p}_s)\}$, where Π denotes the stereographic projection from \mathbb{R}^d to the unit sphere $S^d \subset \mathbb{R}^{d+1}$.
- 2: Compute a centerpoint [32] $\mathbf{c} \in \mathbb{R}^{d+1}$ of $\Pi(\mathcal{P})$, i.e., all hyperplanes containing \mathbf{c} divide the set of points $\{\Pi(\mathbf{p}_1), \Pi(\mathbf{p}_2), \dots, \Pi(\mathbf{p}_s)\}$ in a ratio $(d+1):1$ or less. \mathbf{c} is calculated efficiently by randomly selecting subsets $\mathcal{S} \subset \Pi(\mathcal{P})$ of size $|\mathcal{S}| = a$ and calculating their centerpoints $\mathbf{c}_{\mathcal{S}}$ using Linear Programming on $\mathcal{O}(a^{d+1})$ linear inequalities of $d+1$ variables. (For any $\delta > 0$ this approach produces a $(d+1+\delta):1$ centerpoint with high probability if $a > g(\delta, d+1)$, where g is an s -independent function [33–35], making the approach scalable.)
- 3: Compute an orthogonal matrix $R \in \mathbb{R}^{(d+1) \times (d+1)}$ such that $R\mathbf{c} = (0, 0, \dots, 0, \|\mathbf{c}\|)$.
- 4: Define the dilatation map $D_\alpha = \Pi \circ (\alpha\mathbb{1}) \circ \Pi^{-1}$, where $\alpha = \sqrt{(1 - \|\mathbf{c}\|)/(1 + \|\mathbf{c}\|)}$.
- 5: Choose a random great circle C on S^d . The center of S^d can be shown to be a centerpoint of $D_\alpha \circ R \circ \Pi(\mathcal{P})$ [26], i.e., C divides these points in a ratio $1:(d+1+\delta)$ or better. C gives rise to a sphere $S \subset \mathbb{R}^d$ after transforming back to the original \mathbb{R}^d space, which (generically) satisfies Eq. (2).
- 6: Calculate the sphere $S = \Pi^{-1} \circ R^\top \circ D_\alpha^{-1}(C)$. It can be proven that S also satisfies Eq. (1) with probability at least $1/2$ [26] for sufficiently small $\delta > 0$.
- 7: Check, taking account of the radii \mathcal{R} , if Eqs. (1) and (2) are satisfied. If not, choose another great circle $C' \in S^d$ and repeat steps 5 and 6 until successful. (In general, if any of the above approaches is successful with probability $\rho = \mathcal{O}(1)$, it has to be carried out $1/\rho$ times on average.)

Output: Sphere S , $\Gamma_O(S)$, $\Gamma_E(S)$, $\Gamma_I(S)$.

is applied to: If we go down the separator hierarchy and denote by S_j the sphere with the largest $|\Gamma_O(S)|$ at the j -th level of the separator hierarchy, then in analogy to Eq. (4) the computational time can be bounded according to

$$t(T_0) \leq \sum_{\ell=0}^{z-1} 2^\ell M^{\frac{1}{2} \sum_{j=1}^{2^\ell} |\Gamma_O(S_j)|} + \sum_{m=1}^{2^z} M^{n_m/2}, \quad (6)$$

where n_m denotes the number of constituting tensors contained in the m -th tensor network at the z -th level of the separator hierarchy. In practice, one can also use Eq. (3) directly to obtain a better upper bound for $t(T_0)$.

Finally, we note that for the PST there exists an algorithm to determine the separators in linear time in the number of vertices [31].

V. EXAMPLES

In this Section we consider several examples for which we showcase the strengths of our approach and numerically demonstrate the quantitative advantage of using Algorithm 1. Specifically, we demonstrate that for Google Sycamore-type [17] quantum circuits, the bound of Theorem 2 improves over naive contraction schemes for moderate system sizes. On top of that, Algorithm 1 can be used to obtain massively faster contraction orders, outperforming naive contraction schemes already for small system sizes. Afterwards, we come to the same conclusion for short-range IQP quantum circuits [36], where again Algorithm 1 produces dramatically lower computational costs in practice than the bound of Theorem 2. Finally, we show that the bound of Theorem 2 improves over naive contraction schemes for significantly smaller system sizes than in the previous two examples for $(2+1)$ -dimensional random quantum circuits with Poisson-distributed cavities.

A. Google Sycamore-type quantum circuits

We consider a quantum circuit of the type of Ref. [17] defined on an $L \times L$ lattice of qubits: Each qubit (apart from the edge ones) is acted on by one single-qubit gate and one two-qubit gate coupling it to a nearest neighbor and one two-qubit gate coupling it to a nearest neighbor per “cycle”. There are eight cycles of such couplings, which are repeated periodically (i.e., with two two-qubit gates acting on the same nearest neighbor). We assume that there are q such periods of eight cycles and that in each period a given qubit is inaccessible/ not accessed with a certain probability p , i.e., no single- or two-qubit gate acts on it for the entire period. This induces enough inhomogeneity such that the second bound of Theorem 2 improves over explicit time evolution and the side-wise contraction bound $t_{\text{side}} \leq 2^{4FL}L$ for sufficiently large L . We calculated the corresponding three bounds as a function of system size for $q = 5$ and $p = 0.88$ by averaging over 100 quantum circuit realizations for each L . The results are shown in Fig. 4 and indicate that the bound of Theorem 2 outperforms naive contraction schemes for some (most) quantum circuit realizations for $L \geq 400$ ($L \geq 1600$). Nonetheless, Algorithm 1 outperforms the other contraction schemes at much smaller system sizes than what the bounds of Theorem 2 suggest: In Fig. 4 we also show data for the same parameters as above in the range $4 \leq L \leq 30$ including the upper bounds obtained with Algorithm 1.

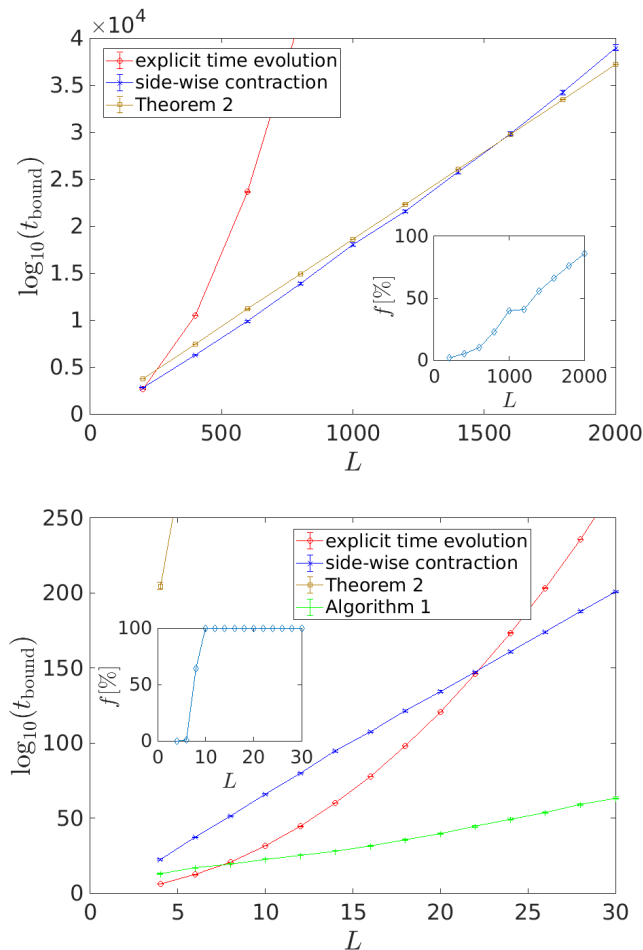


FIG. 4. Top: Mean logarithms of the bounds obtained for the classical computation time based on explicit time evolution ($2^{L^2 - \#(\text{idle qubits})}$), side-wise contraction ($2^{4FL}L$), and the second bound of Theorem 2 averaged over 100 quantum circuit realizations of Sycamore-type quantum circuits. Error bars denote the standard error of the mean of the logarithms. The bound of Theorem 2 improves over explicit time evolution for all realizations for $L \geq 400$ (not shown) and on average over side-wise contraction for $L \geq 1600$. Note that the fraction f of quantum circuits for which Theorem 2 improves over side-wise contraction is non-zero for all considered L , see inset. Bottom: Same as above with the bound from Algorithm 1 added in the range $4 \leq L \leq 30$, with the inset now showing the fraction of quantum circuits for which the bound from Algorithm 1 improves over the computational time of explicit time evolution. (It improves over side-wise contraction for all considered system sizes.)

B. IQP quantum circuits

In this and the following subsection, we employ Algorithm 1 to obtain improved upper bounds on the classical computational complexity of specific quantum circuits using a refined version of Eq. (6), where we explicitly calculate the bond dimensions separating two regions found by the algorithm. Here, we apply the proce-

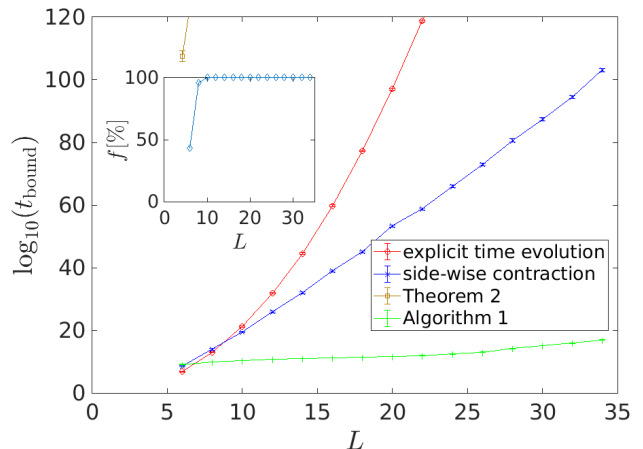


FIG. 5. Mean logarithms of the bounds obtained for the classical computation time based on explicit time evolution ($2^{L^2 - \#(\text{idle qubits})}$), side-wise contraction ($2^{4FL}L$), the second bound of Theorem 2, and the bound obtained with Algorithm 1 averaged over 100 realizations of IQP quantum circuits. Error bars denote the standard error of the mean of the logarithms. Inset: Fraction f of quantum circuits for which the bound from Algorithm 1 improves over side-wise contraction. This bound improves for all realizations over explicit time evolution for $L \geq 8$ (not shown).

cedure to instantaneous quantum polynomial-time (IQP) quantum circuits [36] with single- and two-qubit gates acting on an $L \times L$ lattice of qubits: In each of the T time steps, a single-qubit gate is acted on each qubit with probability $7/8$ [corresponding to randomly chosen phase gates $\text{diag}(1, e^{i\pi m/4})$, $m \in \{0, 1, \dots, 7\}$], and afterwards two-qubit gates act on all nearest-neighbor pairs of qubits which have not yet been acted on in this time step with probability $p = 3/4 \cdot \gamma \ln(N)/N$. The prefactor of $3/4$ corresponds to randomly chosen gates $\text{diag}(1, 1, 1, i^m)$, $m \in \{0, 1, 2, 3\}$. The results for $T = N = L^2$ and $\gamma = 3$ are shown in Fig. 5.

C. (2+1)-dimensional random quantum circuits

We consider an $L \times L$ lattice of qubits and a quantum circuit of $T = \alpha L$ time steps. At each time step, nearest-neighbor gates are densely placed with a random orientation unless there is a cavity in the quantum circuit. These cavities have size $S \times S \times S$ in space-time. Their maximum number v is chosen probabilistically according to a Poisson distribution with parameter λ corresponding to a probability $p_v(\lambda)$. The up to v cavities are placed randomly in the quantum circuit [coordinates (x, y, t)]; each one appears with probability $p(x, y, t) = \exp[-(x^2/L^2 + y^2/L^2 + t^2/T^2)/\sigma^2]$. We choose $S = 5$, $\alpha = 0.1$, $\sigma = 10$, $\lambda = 5 \cdot 10^4(L/200)^{3.5}$ and generate 100 quantum circuits randomly per system size L . The results shown in Fig. 6 indicate that the

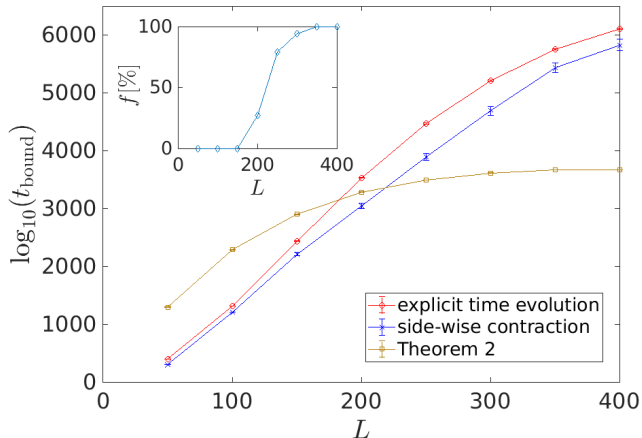


FIG. 6. Mean logarithms of the bounds obtained for the classical computation time based on explicit time evolution ($2^{L^2 - \#(\text{idle qubits})}$), side-wise contraction ($2^{4FL}L$), and the second bound of Theorem 2 averaged over 100 realizations of random quantum circuits with Poisson-distributed numbers of cavities. Error bars denote the standard error of the mean of the logarithms. The bound of Theorem 2 improves over explicit time evolution for all realizations for $L \geq 200$ (not shown) and on average over side-wise contraction for $L \geq 250$. Inset: Fraction f of quantum circuits for which the bound of Theorem 2 improves over side-wise contraction.

bound of Theorem 2 improves over the one for side-wise contraction and explicit time evolution for most quantum circuit realizations for $L \geq 250$ and for a significant fraction already at $L = 200$.

VI. CONCLUSION

We have used the Sphere Separator Theorem to derive analytical upper bounds on the classical contraction runtimes of finite-range higher-dimensional tensor networks. Based on that and the similar Planar Separator Theorem, we proved similar upper bounds for the classical simulation time of arbitrary higher-dimensional quantum circuits with single- and finite-ranged two-qubit gates. We also indicated how the algorithm underlying the SST can be implemented to explicitly determine the contraction order underlying our complexity bound for quantum circuits. While this bound improves over naive contraction schemes only for relatively large system sizes, we showed that, in practice, far better upper bounds are obtained with the Sphere Separator Algorithm, which also yields an estimate for the contraction complexity of a given quantum circuit.

Our approach will find important applications in the context of classical benchmarks for existing quantum simulations and help to determine the regime where they do not meet the criterion of quantum supremacy. We envision particularly powerful classical tensor network contraction schemes as a result of combining our algorithm with other heuristic methods, such as the stem optimization technique of Ref. [20], or the index slicing approach of Ref. [12].

ACKNOWLEDGMENTS

TBW was supported by the ERC Starting Grant No. 678795 TopInSy and the Royal Society Research Fellows Enhanced Research Expenses 2021 RF\ERE\210299. SS acknowledges support from the Royal Society University Research Fellowship.

-
- [1] J. Eisert, *Model. Simu.* **9**, 520 (2013).
 - [2] R. Orús, *Nat. Rev. Phys.* **1**, 538 (2019).
 - [3] L. Tagliacozzo, A. Celi, and M. Lewenstein, *Phys. Rev. X* **4** (2014).
 - [4] P. Silvi, E. Rico, T. Calarco, and S. Montangero, *New J. Phys.* **16**, 103015 (2014).
 - [5] E. Zohar, M. Burrello, T. B. Wahl, and J. I. Cirac, *Ann. Phys.* **363**, 385 (2015).
 - [6] E. Zohar, T. B. Wahl, M. Burrello, and J. I. Cirac, *Ann. Phys.* **374**, 84 (2016).
 - [7] M. C. Bañuls, K. Cichy, J. I. Cirac, K. Jansen, and S. Kühn, *PoS(LATTICE2018)*, **334** (2019).
 - [8] I. L. Markov and Y. Shi, *SIAM J. Comp.* **38**, 963 (2008).
 - [9] A. J. Ferris and D. Poulin, *Phys. Rev. Lett.* **113** (2014).
 - [10] C. Guo, Y. Liu, M. Xiong, S. Xue, X. Fu, A. Huang, X. Qiang, P. Xu, J. Liu, S. Zheng, H.-L. Huang, M. Deng, D. Poletti, W.-S. Bao, and J. Wu, *Phys. Rev. Lett.* **123** (2019).
 - [11] F. Pan, P. Zhou, S. Li, and P. Zhang, *Phys. Rev. Lett.* **125** (2020).
 - [12] C. Huang, F. Zhang, M. Newman, X. Ni, D. Ding, J. Cai, X. Gao, T. Wang, F. Wu, G. Zhang, H.-S. Ku, Z. Tian, J. Wu, H. Xu, H. Yu, B. Yuan, M. Szegedy, Y. Shi, H.-H. Zhao, C. Deng, and J. Chen, *Nat. Comp. Sci.* **1**, 578 (2021).
 - [13] T. Farrelly, R. J. Harris, N. A. McMahon, and T. M. Stace, *Phys. Rev. Lett.* **127** (2021).
 - [14] M. Levental, arXiv:2108.06831.
 - [15] J. C. Napp, R. L. L. Placa, A. M. Dalzell, F. G. Brandão, and A. W. Harrow, *Phys. Rev. X* **12** (2022).
 - [16] E. Stoudenmire and D. J. Schwab, *Adv. Neur. Info. Proc. Sys.* **29**, 4799 (2016).
 - [17] F. Arute, K. Arya, R. Babbush, D. Bacon, J. C. Bardin, *et al.*, *Nature (London)* **574**, 505 (2019).
 - [18] C. Guo, Y. Zhao, and H.-L. Huang, *Phys. Rev. Lett.* **126** (2021).
 - [19] J. Gray and S. Kourtis, *Quantum* **5**, 410 (2021).
 - [20] C. Huang, F. Zhang, M. Newman, J. Cai, X. Gao, Z. Tian, J. Wu, H. Xu, H. Yu, B. Yuan, M. Szegedy, Y. Shi, and J. Chen, arXiv:2005.06787.

- [21] F. Pan, K. Chen, and P. Zhang, arXiv preprint arXiv:2111.03011 (2021).
- [22] F. Pan and P. Zhang, arXiv preprint arXiv:2103.03074 (2021).
- [23] Y. Liu, X. Liu, F. Li, H. Fu, Y. Yang, J. Song, P. Zhao, Z. Wang, D. Peng, H. Chen, *et al.*, in *Proceedings of the International Conference for High Performance Computing, Networking, Storage and Analysis* (2021) pp. 1–12.
- [24] T. Ayril, T. Louvet, Y. Zhou, C. Lambert, E. M. Stoudenmire, and X. Waintal, arXiv:2207.05612.
- [25] R. J. Lipton and R. E. Tarjan, *SIAM Journal on Applied Mathematics* **36**, 177 (1979).
- [26] G. L. Miller, S.-H. Teng, W. Thurston, and S. A. Vavasis, *Journal of the ACM (JACM)* **44**, 1 (1997).
- [27] S. Kourtis, C. Chamon, E. Mucciolo, and A. Ruckenstein, *SciPost Physics* **7** (2019).
- [28] Y. Liu, arXiv:2001.10204.
- [29] C. Huang, M. Newman, and M. Szegedy, *IEEE Transactions on Information Theory* **66**, 5585 (2020).
- [30] W. Smith and N. Wormald, in *Proceedings 39th Annual Symposium on Foundations of Computer Science (Cat. No.98CB36280)* (IEEE Comput. Soc, 1998).
- [31] H. N. Djidjev and S. M. Venkatesan, *Acta Informatica* **34**, 231 (1997).
- [32] H. Edelsbrunner, *Algorithms in Combinatorial Geometry* (Springer Berlin Heidelberg, 1987).
- [33] V. N. Vapnik and A. Y. Chervonenkis, *Theory Prob. Appl.* **16**, 264 (1971).
- [34] D. Haussler and E. Welzl, *Discrete & Computational Geometry* **2**, 127 (1987).
- [35] S.-H. Teng, *Point, Spheres, and Separators: A unified geometric approach to graph partitioning*, Ph.D. thesis, CMU-CS-91-184, School of Computer Science, Carnegie-Mellon Univ., Pittsburgh, Pa. (1991).
- [36] M. J. Bremner, A. Montanaro, and D. J. Shepherd, *Quantum* **1**, 8 (2017).